American Mineralogist, Volume 77, pages 1166–1171, 1992

Kinetics of the marcasite-pyrite transformation: An infrared spectroscopic study

ALISTAIR R. LENNIE, DAVID J. VAUGHAN
Department of Geology, University of Manchester, Oxford Road, Manchester M13 9PL, England

ABSTRACT

The kinetics of the solid-state transformation of marcasite to pyrite have been investigated using infrared spectroscopy. Kinetic analysis using the Johnson-Mehl or Avrami-Erofe'ev equation is based on measurements of infrared absorption intensity made on marcasite samples heated in the temperature range of 698–735 K. From the Arrhenius equation, an activation energy of 253 ± 8 kJ/mol and frequency factor of 4.6×10^{15}/min is calculated for the conversion from marcasite to pyrite. The transformation is modeled by a second-order Johnson-Mehl equation suggesting a nucleation and growth model for the formation of pyrite in the marcasite matrix.

INTRODUCTION

Pyrite and marcasite are naturally occurring phases in the Fe-S system, dimorphs of composition FeS_2. The pyrite crystal structure is cubic (space group *Pa*3), with the octahedrally coordinated Fe atoms at the corners and face centers of the cube unit cell. Disulfide pairs lie at the center of the cube and at the midpoints of the cube edges and are oriented such that their axes are parallel to four nonintersecting body diagonals of the cubic lattice. Each S atom is tetrahedrally coordinated to three Fe atoms and one S atom.

Marcasite has an orthorhombic unit cell (space group *Pnnm*) and, like pyrite, has Fe atoms in octahedral coordination with S, and S atoms tetrahedrally coordinated to three Fe atoms and one S atom. The difference between the marcasite and pyrite structures is found in the linking of the Fe-centered octahedra. In the marcasite structure, these octahedra share two edges in planes normal to (001); in pyrite, the octahedra are linked at corners (Vaughan and Craig, 1978). The pyrite structure can be obtained from that of marcasite by rotation of half of the S_2 groups through 90°.

Marcasite readily inverts to pyrite when heated under vacuum to temperatures above 673 K (Fleet, 1970; Gronvold and Westrum, 1976; Kjekshus and Rakke, 1975). Murowchick and Barnes (1986), in contrast, reported inversion of very fine-grained synthetic marcasite to pyrite at ambient temperatures, and Rising (1973) found that marcasite readily transformed to pyrite above 433 K under hydrothermal reaction conditions. To determine whether marcasite has a field of stability below 673 K, an investigation of the thermodynamic stability of the two iron disulphides utilizing adiabatic-shield calorimetry was made by Gronvold and Westrum (1976). This study demonstrated that marcasite is metastable with respect to pyrite from 5 to 700 K. Above 700 K, marcasite undergoes irreversible exothermic transformation to pyrite.

The difference in ΔG_f^0 values at 298.15 K for marcasite and pyrite is small; for pyrite, $\Delta G_f^0 = -160.060$ kJ/mol, whereas for marcasite, $\Delta G_f^0 = -156.159$ kJ/mol. At 700 K, ΔG_f^0 for pyrite $= -137.074$ kJ/mol, for marcasite, it is -133.617 kJ/mol (Chase et al., 1985), based on the data of Gronvold and Westrum (1976). The formation and persistence of marcasite is thus due not to its thermodynamic stability but to kinetic factors.

Whereas pyrite has been synthesized both by high-temperature reaction between elemental Fe and S and by precipitation from aqueous solution, the synthesis of marcasite has been achieved only by reaction of Fe^{2+} and S species in acidic aqueous solutions (Murowchick and Barnes, 1986; Schoonen and Barnes, 1991a, 1991b, 1991c).

Tossell et al. (1981) proposed that the formation of marcasite from acidic solutions is a function of reaction mechanism. A valence counting scheme suggests that the formation of marcasite in preference to the more stable pyrite (with a system of 14 electron dianions) may be a result of H^+ interaction with the S_2^{2-} dianion electrons. The effect of the H^+ ion is to withdraw two electrons from the metal 3dσ-dianion $1\Pi^*g$ system, giving a distorted geometry to the three Fe atoms coordinated to each S atom of the disulfide group. Loss of H^+ would then expand the M-A-M angle to the value of 97° observed in marcasite.

This model was invoked by Murowchick and Barnes (1986) to interpret experiments that showed a relationship between the pK_1 of the polysulfide solution species and the pH of marcasite formation. Murowchick and Barnes argued that, in acidic solutions, the addition of H_2S_2 to the growing FeS_2 surface results in the marcasite structure. The electron valency of H_2S_2 is effectively the same as that of a 12-electron valent dianion pair. Binding of H_2S_2 to the crystal surface has an electron withdrawing effect that stabilizes the marcasite structure.

In comparison, when HS_n^- is the predominant polysulfide species, it is proposed that the proton has no struc-

0003–004X/92/1112–1166$02.00

turally determining effect, and so the more stable pyrite structure is formed.

Schoonen and Barnes (1991c) concluded from experimental work that the rate of direct nucleation of pyrite and marcasite in slightly acidic solutions is insignificant below 573 K. Instead, most pyrite and marcasite in hydrothermal ores form by sulfidation of iron monosulfide precursors. They interpreted the Murowchick and Barnes (1986) relationship of polysulfide pK to formation pH in terms of surface sulfide species on the growing pyrite or marcasite crystal, rather than in terms of solution sulfide species.

In a crystallographic study (Fleet, 1970) of the structural aspects of the marcasite-pyrite transformation, it was found from X-ray measurements that the inversion to pyrite was partially complete after 12 h at 698 K and essentially complete at 748 K after less than 4 h of heating. Attempts by Kjekshus and Rakke (1975) to detect the inversion using differential thermal analysis (DTA) were, however, unsuccessful.

The present study was undertaken to measure the activation energy of this high-temperature transformation and to determine the mechanism by which this transformation takes place.

Experimental approach

Marcasite samples from the Harwood Mineral Collection of the University of Manchester and pyrite obtained from Manchester Minerals were characterized by X-ray powder diffraction and microprobe analyses.

Analysis of marcasite samples heated in evacuated silica tubes by X-ray powder diffractometry confirmed that transformation to pyrite only occurs over the experimental temperature range. Diffraction peaks corresponding to pyrrhotite were not detected.

To establish the fraction of marcasite transformed to pyrite, a sample of marcasite was coarsely ground in an agate mortar and pestle under amyl acetate. Portions of the ground marcasite were loaded into silica tubes and held in place with silica wool. These silica tubes were then sealed under vacuum, using an O_2-CH_4 flame.

Heating of silica tubes containing the marcasite samples was carried out in a horizontal tube furnace preheated to the required temperature. After the silica tubes were placed in the furnace, the temperature was monitored by a measuring thermocouple close to the end of the silica tube containing the marcasite sample. The measuring thermocouple was calibrated against the melting points of Sn and Pb.

Each tube was removed from the furnace after a timed heating period and immediately quenched in H_2O to halt the inversion reaction. This procedure was carried out at four temperatures (735, 723, 710, and 698 K) and over a range of heating times at each temperature. After the timed heating and quenching process, the marcasite samples were removed from the evacuated silica tubes and ground to a fine powder in a small agate ball mill (Specamill 6000).

Infrared spectroscopy was selected for quantitative analysis of the fraction of marcasite transformed to pyrite. Portions of the milled samples were diluted by adding oven-dried spectral grade KBr in the ratio of 300 parts by weight of KBr to one part by weight of sample. The diluted samples were then thoroughly mixed in the agate mill vessel. Disks were pressed from 200 mg of the sample plus KBr mixture in a Specac 13 mm infrared die at an applied pressure of 9.5 tons. The small ratio of sample to KBr was necessary to avoid high absorption values and thus possible departures from the Beer-Lambert relation in the spectral range of interest.

Standards

To obtain a calibration curve for measurement of the concentration of pyrite and marcasite in the heated samples, a series of pyrite-marcasite standards ranging from 100 wt% marcasite to 100 wt% pyrite were prepared by mixing weighed portions of ground natural samples. These mixtures were ground in the agate ball mill, diluted with KBr in a 1/300 wt ratio, and mixed with KBr in the agate mill. Disks of standard mixtures were pressed from 200 mg of sample as described above. Absorption of moisture was minimized by storage of samples, KBr, and prepared disks in a vacuum desiccator.

Infrared spectra were recorded on a Perkin-Elmer 1710 FTIR spectrometer over the spectral range 4000–220 cm^{-1} with 50 scans per sample at a resolution of 1 cm^{-1}.

Results

The infrared spectra of pyrite and marcasite between 600 and 300 cm^{-1} are shown in Figure 1. The absorption peak of pyrite at 350 cm^{-1} and the marcasite absorption peak at 359 cm^{-1} were selected for measurement of absorption. These peaks are well separated, unlike the more strongly absorbing peaks of marcasite and pyrite in the region of 425 cm^{-1}, which overlap significantly.

Standard mixtures of marcasite and pyrite, ranging from pure marcasite to pure pyrite, were analyzed by the KBr disk method. The absorption intensities were obtained from the recorded spectra by subtraction of the base-line absorbance from the peak absorbance. The base line at the peak wavenumber was established by means of a curve-fitting computer program.

These absorbances have been plotted against the weight percent of the mineral contained in the KBr disk in Figure 2. The plots of absorption intensity values against FeS_2 concentration have been fitted using least-squares linear regression analysis and show a straight-line relationship in accordance with the Beer-Lambert law (Atkins, 1986).

It has been assumed that the disk thickness is the same in all samples, allowing combination of extinction coefficient and path-length terms in the Beer-Lambert law to give the slope of the calibration graph. Disk thicknesses were checked using a micrometer.

The fraction of marcasite converted to pyrite in the heated samples was obtained by measuring absorbances,

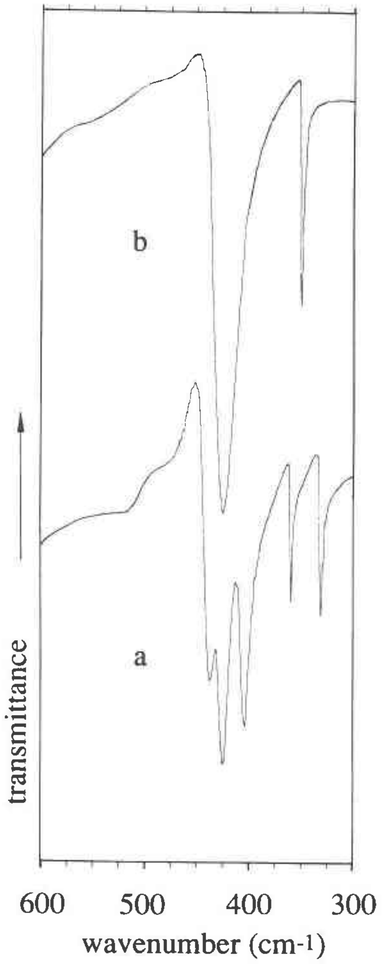

Fig. 1. Infrared transmittance spectra of marcasite and pyrite using iron disulfide incorporated into KBr pressed disks: spectrum a = marcasite, spectrum b = pyrite.

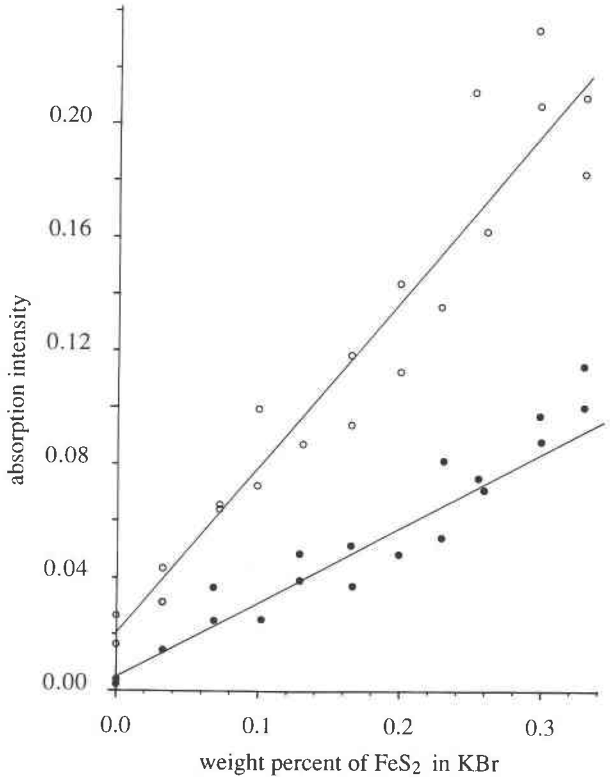

Fig. 2. Calibration graphs for marcasite and pyrite in marcasite + pyrite standard mixtures in KBr disks. Filled circles: absorption of marcasite at $\nu = 359$ cm^{-1} against weight percent marcasite in KBr disks. The marcasite calibration plot has an intercept of 0.005, a slope of 0.275, and a correlation coefficient (r) of 0.93. Open circles: absorption of pyrite at $\nu = 349$ cm^{-1} against weight percent pyrite in KBr disks. The pyrite calibration plot has an intercept of 0.020, slope of 0.590, and correlation coefficient (r) of 0.96.

deriving the weight percent value from the calibration graph, and then calculating the fraction of pyrite (α) from the following relation:

$$\alpha = P/(P + M) \tag{1}$$

where P and M are, respectively, the weight percent of pyrite and weight percent of marcasite measured in the KBr disk. Calculation of α in this way reduces the effect of variations in absorbances due to particle size variations and uneven distribution of iron sulfide in the KBr matrix. The standard error of estimate in α was calculated from differences between prepared and measured fractions of pyrite in the standard mixtures.

From the calibration graphs, the concentrations of marcasite and pyrite in the heated and then quenched samples have been calculated. These analyses are plotted in Figure 3 (as α against ln t).

KINETIC ANALYSIS

It has been found empirically that a rate equation of the form

$$\mathrm{d}\alpha/\mathrm{d}t = K^m t^{m-1}(1 - \alpha) \tag{2}$$

describes the isothermal kinetics of a wide variety of solid-state reactions (Hancock and Sharp, 1972). In addition, many theoretically derived kinetic equations can be reduced to this equation.

Integration and rearrangement of Equation 2 gives

$$\alpha = 1 - \exp[-(k \cdot t)^m] \tag{3}$$

which is known as the Johnson-Mehl or Avrami-Erofe'ev equation. For rate curves conforming to Equation 3, if time is plotted on a logarithmic scale, then the shape of the curve is determined only by m, and k fixes the position on the time axis (Burke, 1965; Redfern, 1987). Figure 3 shows the marcasite transformation data plotted as α against ln t. The curves are of similar shape, indicating similar kinetic behavior.

Reaction curves having the same shape for a range of experimental temperatures are termed isokinetic and have the same value of m if the Johnson-Mehl equation is obeyed. To evaluate m and k, the Johnson-Mehl equation

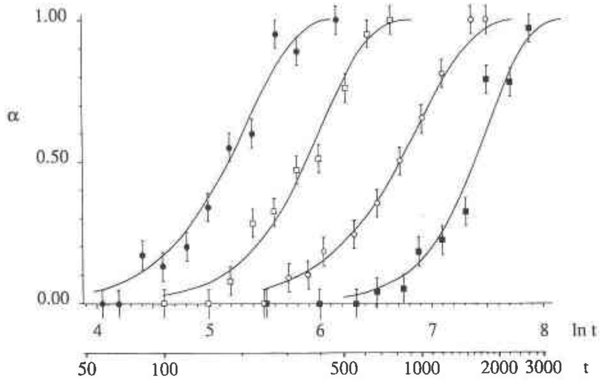

Fig. 3. Fraction of pyrite (α) formed by transformation of marcasite against logarithm of time in minutes. Measurements at 735 K are represented by filled circles, at 723 K by open squares, at 710 K by open circles, and at 698 K by filled squares. The curves are obtained from the Johnson-Mehl equation using values of m and k calculated from experimental data.

is converted to

$$\ln[-\ln(1 - \alpha)] = m \cdot \ln k + m \cdot \ln t \tag{4}$$

by taking logarithms of Equation 3.

A graph of $\ln[-\ln(1 - \alpha)]$ vs. $\ln t$ will be linear if the reaction conforms to the Johnson-Mehl equation. The value of m is obtained from the slope of the graph, and k is derived from the y intercept value from the relation

$$k = \exp(\text{intercept}/m). \tag{5}$$

The data from the experiment are plotted in Figure 4 with $\ln t$ as abscissa and $\ln[\ln(1 - \alpha)]$ as ordinate.

From least-squares linear regression analysis of these plots, values for m and k have been obtained, and they are given in Table 1. These plots show no pronounced curvature, which suggests conformation to the Johnson-Mehl equation throughout the transformation process.

At temperatures of 735, 723, and 710 K, the values for m are similar, indicating that the transformation over this temperature range can be modeled by one kinetic process. Although the value of m derived from the measurements at 698 K is greater than those derived for the higher temperatures, it is proposed that this is a result of experimental variation rather than a fundamental change in reaction mechanism.

With the logarithmic form of the Arrhenius equation,

$$\ln k = \ln \mathrm{A} - E_\mathrm{A}/\mathrm{R}T \tag{6}$$

values of $\ln k$ obtained from the empirical integrated rate equation are plotted against $1/T$ in Figure 5. These give an activation energy, obtained from the gradient ($-E_\mathrm{a}/\mathrm{R}$), of 253 ± 8 kJ/mol, with a frequency factor $A = 4.6 \times 10^{15}$/min.

DISCUSSION

The experimental data presented here are consistent with the previously reported time, temperature, and solid-state transformation results of Fleet (1970) referred to in the introduction. Kjekshus and Rakke (1975) observed that at 573 K, heat treatment under vacuum for up to 14 months does not induce changes in marcasite samples, whereas at 623 K after the same period, mixtures of marcasite and pyrite are obtained. At 673 K, mixtures of marcasite and pyrite are produced after heating for one month.

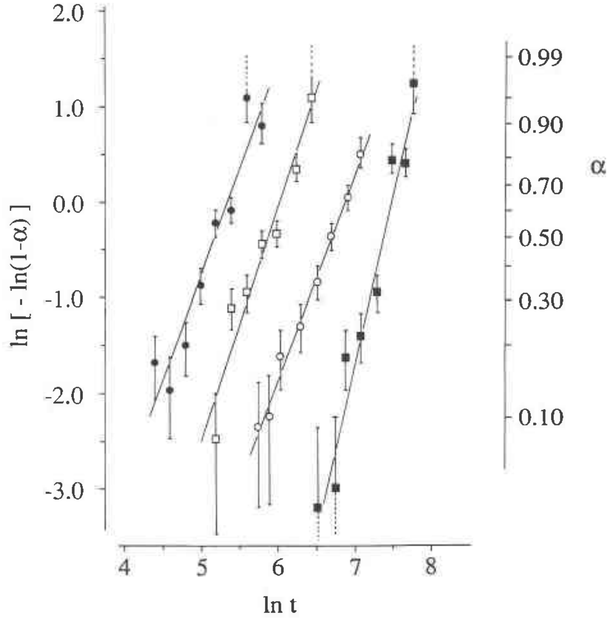

Fig. 4. Plot of ln [$-\ln(1 - \alpha)$] against logarithm of time (in minutes). Measurements at 735 K are represented by filled circles, at 723 K by open squares, at 710 K by open circles, and at 698 K by filled squares.

Estimates of the time taken for a given fraction (α) of pyrite to be produced from marcasite can be made using the activation energy and frequency factor obtained above. A rate constant is derived from the Arrhenius equation for the temperature of interest, and the time taken for a given pyrite fraction (α) to be obtained is calculated from the following form of the Johnson-Mehl equation:

$$t = \langle \exp\{m^{-1} \cdot \ln[-\ln(1 - \alpha)]\} \rangle / k. \tag{7}$$

Calculations using the values of E_a and A derived above and with $m = 2$ suggest that transformation of half of the marcasite to pyrite takes place in approximately 6 d at 673 K, in 205 d at 623 K, and in 40 yr at 573 K.

These estimated values, which should be used as a guide only, are consistent with the reported experimental val-

TABLE 1. Data from plot of $\ln[-\ln(1 - \alpha)]$ against $\ln t$

T (K)	m (slope)	r (correlation coefficient)	k (min^{-1}) (from intercept)
735	2.2 ± 0.3	0.96	0.00475 ± 0.00030
723	2.4 ± 0.3	0.97	0.00238 ± 0.00013
710	2.1 ± 0.3	0.99	0.00101 ± 0.00005
698	2.9 ± 0.3	0.94	0.00054 ± 0.00003

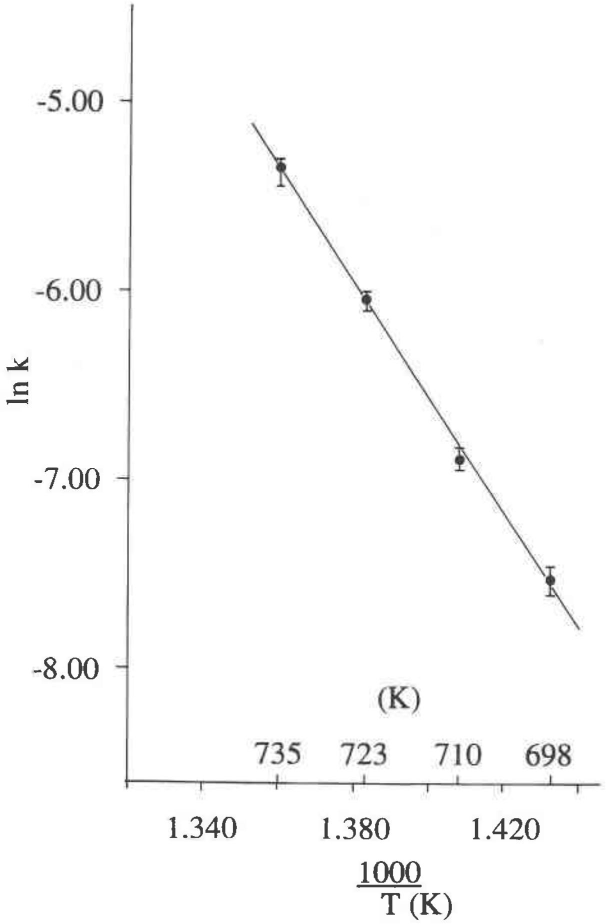

Fig. 5. Arrhenius plot for calculation of the activation energy. Values of k derived from the Johnson-Mehl equation are plotted as ln k against $1000/T$ (K).

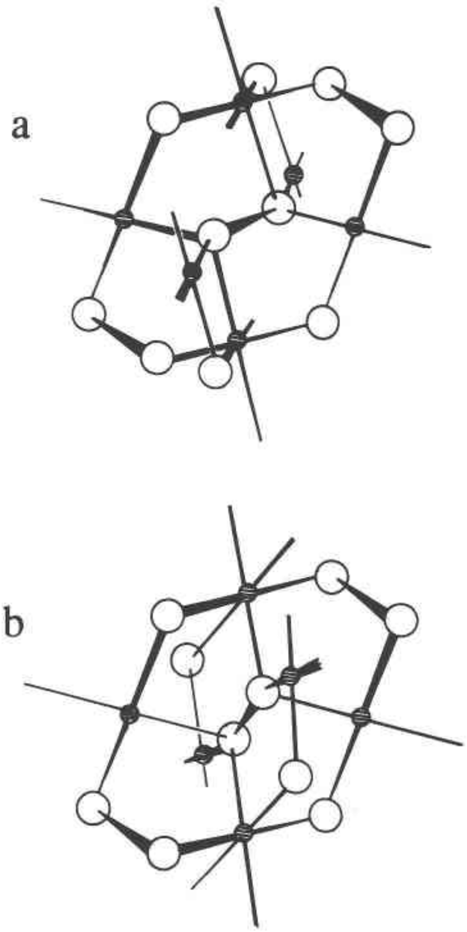

Fig. 6. Model of marcasite (**a**) and pyrite (**b**) structural components showing inversion of the central disulfide pair required to transform marcasite to pyrite. S atoms are represented by the open circles, Fe atoms by the filled circles.

ues of Kjekshus and Rakke (1975). That would suggest that a similar transformation mechanism occurs at lower temperatures, although at considerably slower rates.

Murowchick and Barnes (1986) suggested that the temperature-dependent distribution of marcasite in the Salton Sea geothermal field indicates that temperatures of below 433 K are needed to preserve natural marcasite over a multimillion-year time span. This theory is based on studies by Rising (1973) and McKibbin and Elders (1985).

A half-life for the solid-state transformation of marcasite to pyrite estimated from the above data at 473 K is 3×10^6 yr, whereas at 433 K, calculations give a half-life of 1.3×10^9 yr. These half-lives show a consistency with the proposal of Murowchick and Barnes (1986). Again, these figures should be used with caution, taking note of the limitations of extrapolating higher temperature kinetic data to lower temperatures, and the possible dangers of inferring that the reaction mechanism is the same throughout the temperature range. It is, however, kinetic factors and not thermodynamic stability that ensure long-term preservation of the marcasite structure in natural systems.

If marcasite is slightly S deficient compared with pyrite, as was proposed by Buerger (1934), then ready availability of aqueous S species in hydrothermal systems could speed the transformation to pyrite by a diffusion process (H. L. Barnes, personal communication, 1992).

However, from values of m tabulated by Hancock and Sharp (1972) for various solid-state reactions, the marcasite to pyrite transformation in this experiment corresponds to a nucleation and growth mechanism rather than to a diffusion process. Although Christian (1975) cautioned against proposing a mechanism simply from the value of m obtained in the kinetic analysis of a transformation, examination of the crystal structures of marcasite and pyrite suggests that a nucleation and growth model for the isochemical transformation is more plausible than transformation by diffusion. Furthermore, the suggestion by Fleet (1970) that the structural reorganization involved in the transformation is minimal implies negligible diffusion of Fe and S within the transforming crystal matrix.

A nucleation model is in agreement with the observation that rotation of half of the S_2 groups in marcasite by 90° would result in the pyrite structure (Tossell et al., 1981). This would involve breaking one of the three S-Fe bonds on each end of the disulfide link in order to allow rotation to occur. The Fe-S bonds most likely to break are those forming the four-membered rings arising from edge-sharing octahedra in the marcasite structure. These are the structural features under most strain during heating. Breaking these bonds would allow the S-S group to invert, and new Fe bonds to attach to the S opposite to the former Fe-bonding position on the S (Fig. 6). It is unlikely that the S-S bonds in the structure are broken.

Christian (1975) summarized values of *m* from the Johnson-Mehl equation that describe various models of polymorphic transformations. A value of $m = 2$ corresponds to a grain-edge nucleation model. The pyrite nucleii formed by such a process could then grow along and outward from the marcasite grain edge forming the commonly observed intergrowths (Fleet, 1970) of marcasite {101} parallel to {001} of pyrite.

ACKNOWLEDGMENTS

Thanks are due to Dennis Rawlinson of the Chemistry Department, Manchester University, for valuable assistance with the infrared analysis. Discussions with Simon Redfern on collection and analysis of kinetic data provided an important input to this work. We thank H.L. Barnes for his constructive review, which helped to clarify interpretation of the data. This project was supported by NERC grant GR3/6823 A.

REFERENCES CITED

Atkins, P.W. (1986) Physical chemistry (3rd edition). Oxford University Press, Oxford, England.

Buerger, M.J. (1934) The pyrite-marcasite relation. American Mineralogist, 19, 37–61.

Burke, J. (1965) The kinetics of phase transformations in metals. Pergamon Press, Oxford.

Chase, M.W., Jr., Davies, C.A., Downey, J.R., Jr., Frurip, D.J., McDonald, R.A., and Syverud, A.N. (1985) JANAF thermochemical tables. Journal of Physical and Chemical Reference Data, 14, 1198–1199.

Christian, J.W. (1975) The theory of transformations in metals and alloys. Part 1: Equilibrium and general kinetic theory (2nd edition). Pergamon Press, Oxford, England.

Fleet, M.E. (1970) Structural aspects of the marcasite-pyrite transformation. Canadian Mineralogist, 10, 225–231.

Gronvold, F., and Westrum, E.F., Jr. (1976) Heat capacities of iron disulfides. Thermodynamics of marcasite from 5 to 700 K, pyrite from 300 to 780 K, and the transformation of marcasite to pyrite. Journal of Chemical Thermodynamics, 8, 1039–1048.

Hancock, J.D., and Sharp, J.H. (1972) Method of comparing solid-state kinetic data and its application to the decomposition of kaolinite, brucite and $BaCO_3$. Journal of the American Ceramic Society, 55, 74–77.

Kjekshus, A., and Rakke, T. (1975) Compounds with marcasite type crystal structure. XI. High temperature studies of chalcogenides. Acta Chemica Scandinavica A, 29, 443–452.

McKibbin, M.A., and Elders, W.A. (1985) Fe-Zn-Cu-Pb mineralization in the Salton Sea geothermal system, Imperial Valley, California. Economic Geology, 80, 539–559.

Murowchick, J.B., and Barnes, H.L. (1986) Marcasite precipitation from hydrothermal solutions. Geochimica et Cosmochimica Acta, 50, 2615–2629.

Redfern, S.A.T. (1987) The kinetics of dehydroxylation of kaolinite. Clay Minerals, 22, 447–456.

Rising, B.A. (1973) Phase relations among pyrite, marcasite, and pyrrhotite below 300 °C, 192 p. Ph.D. thesis, Pennsylvania State University, University Park, Pennsylvania.

Schoonen, M.A.A., and Barnes, H.L. (1991a) Reactions forming pyrite and marcasite from solution: I. Nucleation of FeS_2 below 100 °C. Geochimica et Cosmochimica Acta, 55, 1495–1504.

——— (1991b) Reactions forming pyrite and marcasite from solution: II. Via FeS precursors below 100 °C. Geochimica et Cosmochimica Acta, 55, 1505–1514.

——— (1991c) Mechanisms of pyrite and marcasite formation from solution: III. Hydrothermal processes. Geochimica et Cosmochimica Acta, 55, 3491–3504.

Tossell, J.A., Vaughan, D.J., and Burdett, J.K. (1981) Pyrite, marcasite, and arsenopyrite type minerals: Crystal chemical and structural principles. Physics and Chemistry of Minerals, 7, 177–184.

Vaughan, D.J., and Craig, J.R. (1978) Mineral chemistry of metal sulfides. Cambridge University Press, Cambridge, England.

MANUSCRIPT RECEIVED JANUARY 13, 1992
MANUSCRIPT ACCEPTED JUNE 25, 1992